Supplementary Information:
Functionalized terahertz plasmonic metasensors:
Femtomolar-level detection of SARS-CoV-2 spike proteins

Arash Ahmadivand,[1,2]†* Burak Gerislioglu,[3]† Zeinab Ramezani,[4] Ajeet Kaushik,[5] Pandiaraj Manickam,[6,7] and S. Amir Ghoreishi[8]

[1]*Department of Electrical and Computer Engineering, Rice University, 6100 Main St, Houston, Texas 77005, United States*

[2]*Metamaterial Technologies Inc. Pleasanton, CA 94588, United States*

[3]*Department of Physics and Astronomy, Rice University, 6100 Main St, Houston, Texas 77005, United States*

[4]*Department of Electrical and Computer Engineering, Northeastern University, Boston, MA 02115, United States*

[5]*NanoBioTech Laboratory, Department of Natural Sciences, Division of Sciences, Art, & Mathematics, Florida Polytechnic University, Lakeland, Florida 33805, United States*

[6]*Electrodics and Electrocatalysis Division, CSIR-Central Electrochemical Research Institute (CECRI), Karaikudi 630 003, Tamil Nadu, India*

[7]*Academy of Scientific & Innovative Research (AcSIR), Ghaziabad 201 002, Uttar Pradesh, India*

[8]*Faculty of Electrical & Computer Engineering, Science and Research Branch, Islamic Azad University of Tehran, Tehran, Iran*

arash.ahmadivand@metamaterial.com

†: Equal contribution

1. Functionalized Gold Nanoparticles

We utilized NHS dried colloidal gold nanoparticles with the average size of 45 nm. The size distribution of nanoparticles is demonstrated in Figure S1.

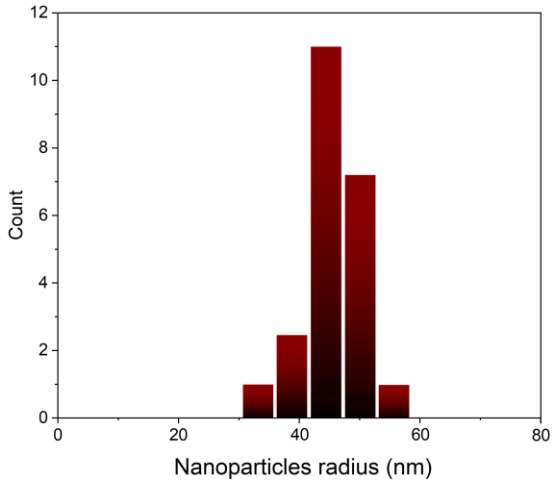

Figure S1. Size distribution of gold nanoparticles.

2. Geometry of the unit cell

The important geometrical parameters of the terahertz (THz) plasmonic metamolecule are given in Figure S2. As critical components in the formation of toroidal moment, we focused our electromagnetic and experimental analyses on the optimization of the capacitive gaps (g) and distance (D) between proximal resonators. Ultimately, we defined the geometric parameters as following: $W/L/D/g$= 15/90/10/5 μm. The

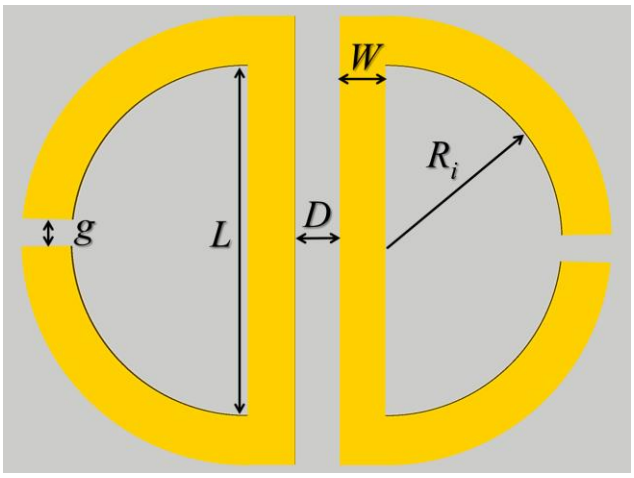

Figure S2. Important geometric parameters of the unit cell (top-view).

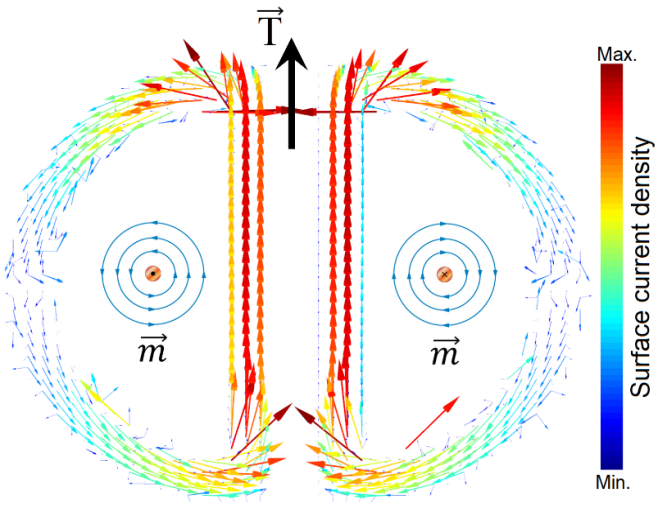

Figure S3. Vectorial surface current density map for the toroidal mode at the resonance frequency in *x-y* plane.

inner radius of the broken half-rings was set to R_i=45 μm and the entire thickness of the metastructure was set to 300 nm, homogenously.

3. Fabrication of the Toroidal Metadevice

The designed metasurface composed of metallic unit cells were developed by conventional single-step photolithography technique on an undoped high-resistive (>10000 Ω.cm) silicon substrate with the crystal orientation of <100> and thickness of 500 μm to provide the required transparency in the THz spectrum.[1,2] Prior to fabrication process, the wafers were sonicated in acetone for 10 min, rinsed with isopropyl alcohol (IPA) and deionized (DI) water, and then dried by Nitrogen gas. We employed a negative photoresist (NLOF 2020) with the total thickness of 2 μm to develop the patterns. Utilizing the e-beam metallization tool, we deposited 300 nm of gold layer at the rate of 1 Å/s (pressure 2×10^{-4} mTorr), followed by a lift-off process in Acetone for 20 min.

4. Measurement and Characterization of Samples

The THz characterization was performed using a THz time-domain spectroscopy (THz~TDS) setup with the beam bandwidth of f~0.2 THz to 4.5 THz, the frequency resolution of 200 GHz, and a signal-to-noise (S/N) ratio of over 10,000:1. More precisely, for the generation of broadband THz beams, we used a Ti:S femtosecond oscillator with the pulse width of 100 fs. The dominant wavelength and average power of the

oscillator were set to 850 nm and 1.5 W, respectively. The pulsed laser beam was focused onto a biased GaAs THz emitter. The propagating terahertz radiation was detected electro-optically using a ZnTe crystal.

5. Calculations and Theoretical Modeling

Throughout, we used finite-difference time-domain (FDTD, Lumerical 2020) to accurately predict and study the electromagnetic response of the THz toroidal-resonant metadevice by solving Maxwell's equations. For the optical computations, the simulation area discretization was set to dx=dy=25 nm in x- and y-planes, and dz=10 nm in z-axis. Perfectly matched layer (PML) boundaries with 64 layers encompassed the workplace along the beam propagation direction (z-axis) and symmetric–antisymmetric periodical boundaries were employed for x- and y-trajectories. To satisfy the Courant stability, we set the simulation time step to dt~ 0.1 fs. In addition, the dielectric functions for the gold unit cells were taken from empirically reported constants and the complex refractive index was set to n=400+i600.[3] The current density profile in Figure S3 was calculated using the displacement current module based on implementing the effective permittivity of the system ($\vec{\boldsymbol{D}} = \boldsymbol{\varepsilon_{eff}}\vec{\boldsymbol{E}}$). Subsequently, the current density was solved in FDTD simulations using the following equation: $\vec{\boldsymbol{J}} = -\boldsymbol{i\omega}\left(\boldsymbol{\varepsilon_{ff}} - \boldsymbol{\varepsilon_0}\right)\vec{\boldsymbol{E}}$.[4] Figure S3 also demonstrates the explicit discrepancy between the directions of the spinning magnetic moments, validating the formation of a destructive interference and subsequently excitation of a toroidal dipole moment.

References

[1] J. Grzyb, and U. Pfeiffer, THz direct detector and heterodyne receiver arrays in silicon nanoscale technologies. *J. Infrared Millim. THz Waves* 36 (10), 998-1032 (2015).

[2] B. Gerislioglu, A. Ahmadivand, and N. Pala, Tunable plasmonic toroidal terahertz metamodulator. *Phys. Rev. B* 97(16), 161405 (2018).

[3] G. Scalari, C. Maissen, D. Turčinková, D. Hagenmüller, S. De Liberato, C. Ciuti, C. Reichl, D. Schuh, W. Wegscheider, M. Beck, and J. Faist, Ultrastrong coupling of the cyclotron transition of a 2D electron gas to a THz metamaterial. *Science* 335(6074), 1323-1326 (2012).

[4] A. Ahmadivand, B. Gerislioglu, and Z. Ramezani, Generation of magnetoelectric photocurrents using toroidal resonances: a new class of infrared plasmonic photodetectors. *Nanoscale* 11(27), 13108-13116 (2019).